and transient absorption experiments which demonstrate that the excited states of three Ru(II) complexes, (Chart I) tris(2,2′-bipyridyl)ruthenium(II) dichloride (I), tris(1,10-phenanthroline)ruthenium(II) dichloride (II), and tris(4,7-diphenyl-1,10-phenanthroline)ruthenium(II) dichloride (III), are indeed localized on the ligand.

Presented in Figure 1 are the excited-state absorption spectra for I–III recorded 10 ns after Nd:YAG laser excitation at 354.5 nm, uncorrected for the ground-state absorption.[8] The transient excited-state absorption spectrum of I is considerably red shifted compared to those of II and III. These difference spectra clearly show that the excited state of I absorbs more at 354.5 nm than those of II and III. The ground states of all of the complexes possess very little absorbance at 354.5 nm. As a result, the excited states of II and III should show less resonance enhancements at this wavelength than that of I. This is probably a contributing factor to the absence of reports of the TR^3 spectrum of II in the literature. The excited-state resonance Raman spectra of II and III, along with that of I, are shown in Figure 2.

With sodium sulfate (0.5 M) used as an internal standard, the Raman intensities of I and II were compared and the lines in the spectrum of II were found to be *at least 5–6 times weaker* than that those in the spectrum of I. Increasing the pulse energies up to 40 mJ did not produce significant differences in the spectra, consistent with saturation of excited-state population, under pulsed excitation conditions. For comparison, the ground-state resonance Raman (RR) spectra of these complexes were measured,[9] and these frequencies are listed in Table I.

The TR^3 spectra of I–III are quite distinct from the corresponding ground-state spectra. Thus, all the available evidence is consistent with the assignment of the TR^3 spectra shown in Figure 2 to the triplet electronically excited states of I–III. The TR^3 spectrum of II is considerably different from the ground-state spectrum of II obtained by 441.6-nm excitation (or 325-nm excitation). The ground-state spectrum obtained at 350.7 nm is also different from the excited-state spectrum.[9] The differences in the TR^3 spectra of I–III are attributed to electron localization on different ligands associated with the metal center.[10]

In conclusion, the TR^3 spectra of II and III have been obtained for the first time. The excited-state spectrum of II is extremely weak, which is at least in part due to the low extinction coefficient for the excited state at 354.5 nm (Figure 1). On the basis of earlier assignments of the TR^3 spectra of ruthenium complexes[4,5] we suggest that these states are also ligand-localized MLCT states. The striking dissimilarities among the spectra of I–III, open the possibility of investigation of the electronic nature of the excited states of the mixed chelates of Ru(II) containing these ligands, of probing the relative distributions of the excited-state electron on different ligands, and of the study of electron hopping from ligand to ligand within the same complex. The results of these investigations will be reported shortly.

Acknowledgment. The authors thank Drs. M. B. Zimmt and M. Paczkowski for their outstanding assistance in the design and construction of the Raman spectrometer. For helpful discussions and for copies of the 350.7-nm excitation Raman spectra of II, Dr. W. H. Woodruff (Los Alamos) is gratefully acknowledged. We also thank the National Science Foundation and the Army Research Office for their generous support of this work.

Registry No. Ru(bpy)$_3^{2+}$, 15158-62-0; Ru(phen)$_3^{2+}$, 22873-66-1; Ru(DIP)$_3^{2+}$, 63373-04-6.

Supplementary Material Available: Figure 3, ground-state resonance Raman spectra of I–III (1 page). Ordering information is given on any current masthead page.

---

(8) The samples were excited perpendicular to the monitoring light beam. The spectra with and without laser excitation were collected after dispersion through an ISA HR-320 spectrograph and PARC OMA-111 detector. The spectrograph was calibrated with mercury emission lines.

(9) For some of the ground-state RR spectra see: Bradley, P. G. Ph.D. Thesis, The University of Texas at Austin, 1982. Basu, A.; Gafney, H. D.; Strekas, T. C. *Inorg. Chem.* **1982**, *21*, 2231. For excited-state spectral correlations, see: McClanaham, S. F.; Dallinger, R. F.; Holler, F. J.; Kincaid, J. R. *J. Am. Chem. Soc.* **1985**, *107*, 4853.

(10) We were unable to obtain the resonance Raman spectrum of the phen radical ion due to its instability under our experimental conditions. To the best of our knowledge, the resonance Raman spectrum of this species has not been reported in the literature. If our assignment of the TR^3 spectrum of II is correct, then the spectrum shown in Figure 2 can serve as a basis for construction of the resonance Raman spectrum of II.

Contribution from DRF/LCH (UA 1194),
Centre d'Etudes Nucléaires de Grenoble, F 85X,
38041 Grenoble Cedex, France, and Department of Chemistry,
University of Surrey, Guildford GU2 5XH, U.K.

X-ray Structural Characterization and Magnetic Properties of a Novel Tetranuclear Copper Catecholate

Eric Gojon,[†] Stephen J. Greaves,[‡] Jean-Marc Latour,*[†]
David C. Povey,*[‡] and Gallienus W. Smith[‡]

Received July 24, 1986

The interaction of catechols with transition-metal ions has attracted much recent interest[1] due to its biological relevance as well as its possible involvement in synthetic procedures. Several copper complexes of catechols[2–9] and semiquinones[9–11] have been studied in this context; however, structural characterizations of these kinds of compounds have only appeared in the very recent past,[7,9,11] and in all but one case,[7] chelating catechols or semiquinones were observed. As part of a project aimed at synthesizing multinuclear complexes of redox-active ligands, we investigated the possibility of binding catechols in a new unsymmetrical (nonchelating) mode in order to use the other (or both) oxygen(s) to complex a second metal ion. In this report we describe the structural and magnetic properties of a tetranuclear copper bis(catecholato) complex in which each catecholate is bound to three copper atoms of a tetranuclear cluster and exhibits both the chelating and two different bridging bonding modes.

The catechol ligands (H_2L) are prepared by condensation of 2,3-dihydroxybenzaldehyde with the corresponding (aminoalkyl)pyridine as unstable off-white solids. The various complexes are obtained upon reacting an ethanol solution of the ligand with the chosen copper salt and recrystallizing the resulting green (or brown in the case of the acetates) powder from methanol. The X-ray structure of $[Cu_2(L_2)_2(CH_3CO_2)_2]_2 \cdot H_2O$ (**4**) was determined on pale brown crystals that formed upon slow evaporation of a methanol solution.[12]

The structure of the complex is shown in Figure 1.[13,14] The molecule is composed of two halves related by a center of symmetry located at the center of the Cu2O1Cu2′O1′ parallelogram. Each half of the molecule is constituted by a dicopper unit where the metal atoms are bridged by the ligand and two acetate ions. The symmetry around Cu1 is close to a trigonal bipyramid with the pyridine nitrogen N2 and the bridging oxygen O2 from the catechol occupying the axial positions of the bipyramid. On the other hand, the environment of Cu2 approaches a square pyramid whose basal plane comprises an acetate oxygen O4 and three oxygens from the catechols, and the apical position is occupied by a fifth oxygen, O6, from a different acetate. The Cu1···Cu2 distance within this dinuclear moiety is 3.303 Å. This distance is longer than the Cu2···Cu2′ distance (3.053 Å) observed between the two dinuclear units. The reason for this lies in the fact that in the latter case only one-atom bridges are involved while two three-atom bridges (acetate) are present in the former. Finally, it is to be noted that mean C–O and C–C bond lengths are 1.33 and 1.41 Å, respectively, which supports the copper(II)–catecholate formulation.[1,9]

The bonding mode exhibited by the catecholate in the dinuclear units of **4** is exactly the one proposed to occur in an intermediate

---

[†] Centre d'Etudes Nucléaires de Grenoble.

[‡] University of Surrey.

Chart I

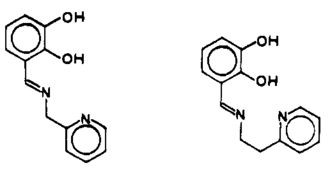

$H_2(L_1)$ $H_2(L_2)$

$Cu(HL_1)(NO_3)\cdot H_2O$ (**1**)
$Cu(HL_1)Cl\cdot H_2O$ (**2**)
$[Cu_2(L_1)(CH_3CO_2)_2]_2\cdot 3H_2O$ (**3**)
$[Cu_2(L_2)(CH_3CO_2)_2]_2\cdot H_2O$ (**4**)

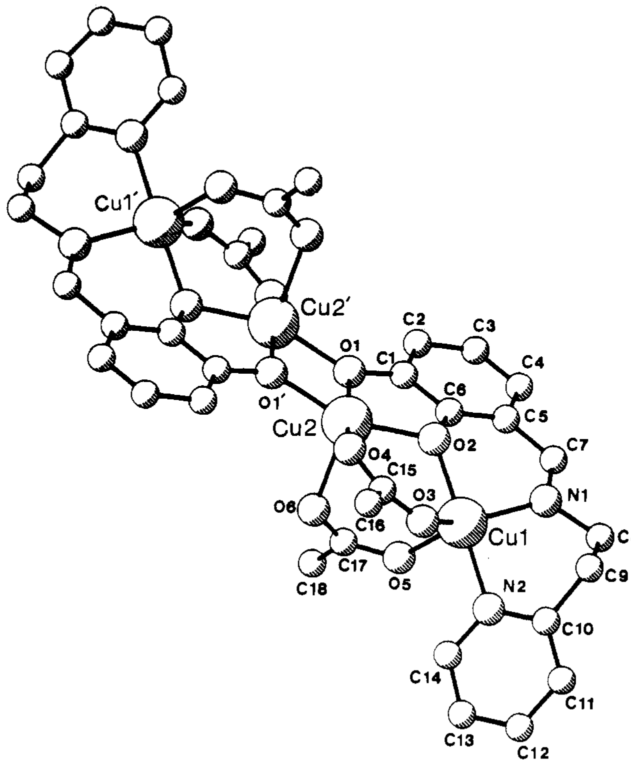

Figure 1. Structure of **4**. Selected bond lengths (Å) and angles (deg): Cu1–Cu2 = 3.303 (1), Cu2–Cu2′ = 3.053 (1), Cu1–N2 = 2.010 (4), Cu1–O2 = 1.933 (3), Cu1–N1 = 2.009 (4), Cu1–O3 = 2.058 (4), Cu1–O5 = 2.096 (4), Cu2–O1 = 1.934 (4), Cu2–O2 = 1.976 (3), Cu2–O4 = 1.913 (4), Cu2–O1′ = 1.965 (4), Cu2–O6 = 2.181 (5), C1–O1 = 1.346 (6), C6–O2 = 1.353 (6), C1–C6 = 1.407 (7); N2–Cu1–O2 = 177.1 (2), N2–Cu1–N1 = 92.2 (2), N2–Cu1–O3 = 85.4 (2), N2–Cu1–O5 = 90.9 (2), O2–Cu1–N1 = 89.6 (2), O2–Cu1–O3 = 91.7 (2), O2–Cu1–O5 = 90.4 (2), N1–Cu1–O3 = 133.9 (2), N1–Cu1–O5 = 115.4 (2), O3–Cu1–O5 = 110.7 (2), O6–Cu2–O1 = 100.6 (2), O6–Cu2–O1′ = 102.5 (2), O6–Cu2–O2 = 93.7 (2), O6–Cu2–O4 = 95.8 (2), O1–Cu2–O1′ = 76.9 (2), O1–Cu2–O2 = 83.6 (1), O1–Cu2–O4 = 163.4 (2), O1′–Cu2–O2 = 156.6 (2), O1′–Cu2–O4 = 96.9 (2), O2–Cu2–O4 = 98.2 (2), Cu2–O1–Cu2′ = 103.1 (0).

Table I. Atomic Coordinates with Estimated Deviations for $[Cu_2L_2(CH_3CO_2)_2]_2\cdot H_2O$

atom	*x*	*y*	*z*
Cu1	0.36821 (8)	0.63671 (6)	0.68179 (5)
Cu2	0.51899 (8)	0.90948 (6)	0.59129 (5)
O1	0.3923 (5)	0.9116 (4)	0.4408 (3)
O2	0.4248 (4)	0.7097 (4)	0.5586 (3)
O3	0.5920 (5)	0.7241 (4)	0.7884 (3)
O4	0.6947 (5)	0.9003 (4)	0.7190 (3)
O5	0.1884 (5)	0.7763 (4)	0.6839 (4)
O6	0.3410 (6)	0.9757 (5)	0.6845 (4)
O7	0.500	0.000	0.000
N1	0.2882 (6)	0.4490 (4)	0.5832 (4)
N2	0.3213 (6)	0.5645 (4)	0.8147 (4)
C1	0.3010 (7)	0.7880 (5)	0.3916 (4)
C2	0.1986 (7)	0.7623 (6)	0.2844 (4)
C3	0.1108 (7)	0.6304 (6)	0.2425 (5)
C4	0.1232 (7)	0.5254 (6)	0.3052 (5)
C5	0.2256 (7)	0.5495 (6)	0.4139 (4)
C6	0.3172 (6)	0.6804 (5)	0.4565 (4)
C7	0.2314 (8)	0.4360 (6)	0.4789 (5)
C8	0.2798 (9)	0.3199 (6)	0.6330 (5)
C9	0.3999 (8)	0.3386 (6)	0.7461 (5)
C10	0.3450 (7)	0.4318 (6)	0.8328 (5)
C11	0.3212 (8)	0.3886 (6)	0.9289 (5)
C(12)	0.2720 (8)	0.4803 (7)	1.0064 (5)
C13	0.2483 (8)	0.6133 (7)	0.9864 (5)
C14	0.2717 (8)	0.6515 (6)	0.8896 (5)
C15	0.6992 (7)	0.8204 (6)	0.7893 (5)
C16	0.853 (1)	0.8485 (8)	0.8850 (6)
C17	0.2074 (8)	0.9049 (6)	0.6779 (5)
C18	0.058 (1)	0.9737 (9)	0.660 (1)

active in catechol oxidation.[15] In this respect, it is worth noting that **4** and the other complexes in this study are perfectly air-stable. This is not surprising since the imine function certainly lowers the catechol oxidizability. However, a ligand oxidation is easily observed by electrochemical methods.[16]

The acetate derivative of H_2L_1, **3**, possesses probably the same structure as **4**, since the two compounds exhibit almost identical spectroscopic and magnetic properties. On the other hand, the nitrate and chloride derivatives of H_2L_1, **1** and **2**, respectively, behave in a manner similar to that of their salicylaldehyde analogues.[17] This suggests that the copper atom is bound in the N_2O coordination site provided by the ligand. This conclusion is further supported by the observation that both compounds lack the 1267 cm^{-1} infrared absorption found in the acetates that is characteristic of the chelated copper catecholate structure.[2] Through the use of FTIR difference spectra (with **2** as a basis) it has been possible to locate the vibrations of the acetate and nitrate ligands of the H_2L_1 derivatives. These occur at 1435–1587 and 1354–1418 cm^{-1}, confirming the bridging nature[18] of the acetate and suggesting

---

(1) Pierpont, C. G.; Buchanan, R. M. *Coord. Chem. Rev.* **1981**, *38*, 45–87.

(2) Brown, D. G.; Reinprecht, J. T.; Vogel, G. C. *Inorg. Nucl. Chem. Lett.* **1976**, *12*, 399–404.

(3) Kwik, W. L.; Ang, K. P. *Aust. J. Chem.* **1978**, *31*, 459–463.

(4) Rogic, M.; Demmin, T. R. *J. Am. Chem. Soc.* **1978**, *100*, 5472–5487.

(5) Andra, K.; Fleischer, F. *Z. Anorg. Allg. Chem.* **1982**, *485*, 210–216.

(6) Harmalker, S.; Jones, S. E.; Sawyer, D. T. *Inorg. Chem.* **1983**, *22*, 2791–2794.

(7) Karlin, K. D.; Gultneh, Y.; Nicholson, T.; Zubieta, J. *Inorg. Chem.* **1985**, *24*, 3725–3727.

(8) Balogh-Hergovich, E.; Speier, G. *Inorg. Chim. Acta* **1985**, *108*, 59–62.

(9) Buchanan, R. M.; Wilson,-Blumenberg, C.; Trapp, S. K.; Greene, D. L.; Pierpont, C. G. *Inorg. Chem.* **1986**, *25*, 3070–3076.

(10) Muraev, V. A.; Cherkasov, V. K.; Abakumov, G. A.; Razuvaev, G. A. *Dokl. Akad. Nauk SSSR* **1977**, *236*, 620–623.

(11) (a) Thompson, J. S.; Calabrese, J. C. *Inorg. Chem.* **1985**, *24*, 3167–3171. (b) Thompson, J. S.; Calabrese, J. C. *J. Am. Chem. Soc.* **1986**, *108*, 1903–1907.

(12) Anal. Calcd for $C_{36}H_{38}N_4O_{13}Cu_4$: C, 43.73; H, 3.87; N, 5.67. Found: C, 43.4; H, 4.0; N, 5.5. All other compounds give satisfactory analyses, which have been supplied to the reviewers.

(13) The complex **4** crystallizes in the space group $P\bar{1}$ with two molecules per unit cell: $a = 8.365$ (2) Å, $b = 9.667$ (1) Å, $c = 12.556$ (1) Å, $\alpha = 98.40$ (2)°, $\beta = 103.97$ (2)°, $\gamma = 94.26$ (2)°. Intensities of 4075 reflections with $(\sin\theta)/\lambda \leq 0.62$ were measured on an Enraf-Nonius CAD4 diffractometer using graphite-monochromated Mo Kα radiation. A total of 1038 reflections with $I < 3.0\sigma(I)$ were classified as unobserved. The structure was solved by the heavy-atom technique and refined by full-matrix least squares to $R = 0.044$. Non-hydrogen atoms were allocated anisotropic thermal parameters; hydrogen atoms were allocated fixed thermal parameters, $B = 5.0$ Å^2. Omitting the water oxygen atom O7 results in a 3.1% increase in the *R* factor. The high *B* factor is indicative of disorder, but the occupancy was not refined. Table I lists the atomic positional parameters.

(14) Supplementary material.

(15) Demmin, T. R.; Swerdloff, M. D.; Rogic, M. M. *J. Am. Chem. Soc.* **1981**, *103*, 5795–5804.

(16) In dimethylformamide all complexes present in cyclic voltammetry an oxidation peak near 0.8 V vs. SCE. This irreversible process requires four electrons and leads to ligand destruction and copper release.

(17) Latour, J. M.; Leonard, G. A.; Limosin, D.; Povey, D. C.; Tandon, S. S. In *Biological and Inorganic Copper Chemistry*; Karlin, K. D., Zubieta, J., Eds.; Adenine: New York, 1985; pp 221–230.

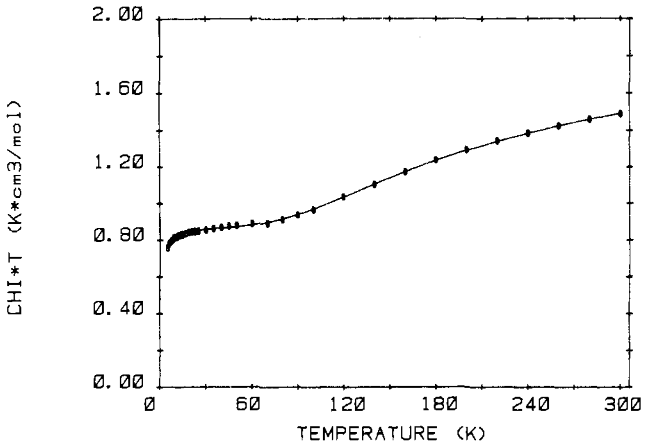

Figure 2. Temperature dependence of the magnetic susceptibility under the form of the χT vs. T curve: (O) experimental points; (—) theoretical curve. The theoretical curve is calculated from the equation below, with

$$\chi_{\text{calcd}} = \frac{N\beta^2 g_1^2}{2k(T-\Theta)} + \frac{2N\beta^2 g_2^2}{3kT}\left[1 + \frac{1}{3}e^{-2J/kT}\right] + 2N\alpha$$

the following "best-fit parameters": $g_1 = 2.16$, $\Theta = -0.75$ K, $g_2 = 2.18$, $-2J = 259$ cm^{-1}, $2N\alpha = 2.4 \times 10^{-4}$ cm^3/mol. The quantity minimized in the least-squares process was $Q = \sum[\chi_{\text{exptl}}T - \chi_{\text{calcd}}T]^2$. The final value of the statistical index $R = Q/N\sum[\chi_{\text{exptl}}T]^2$ was 3.0×10^{-7}.

that the nitrate is monodentate[18] as it is in the salicylaldehyde analogue.[17]

Figure 2 illustrates the magnetic properties of **4** in the form of the χT vs. T curve over the range 5–300 K. This curve exhibits two domains: First, a plateau at $\chi T = 0.8$ K cm^3/mol for temperatures lower than ca. 60 K is indicative of the presence of two independent spins $S = {}^1/_2$. Second, the increase of χT in the upper temperature range reveals an antiferromagnetically coupled system that starts contributing at temperatures higher than 60 K. These properties can be nicely accounted for if one considers that the tetranuclear complex is constituted by two Curie-behaved ions and a binuclear moiety. Fitting the curve under the above assumptions leads to a singlet–triplet separation of 259 cm^{-1} for the dinuclear unit, which is a moderately high value. This model is consistent with Cu2 and Cu2′ forming the coupled pair and Cu1 and Cu1′ being the isolated ions. Owing to the tetragonal symmetry around Cu2 and Cu2′ the magnetic orbitals of each metallic fragment will be of $d_{x^2-y^2}$ type, thus providing a good overlap on the oxygen atoms O1 and O1′. Moreover, by analogy with hydroxy-[19] and alkoxy-bridged[20] complexes, the high value of the Cu2–O1–Cu2′ angles (103°) predicts a significant coupling, in agreement with the observation. At first glance, a coupling could also be predicted between Cu1 and Cu2 since the magnetic orbitals on Cu1 (d_{z^2}) and on Cu2 ($d_{x^2-y^2}$) would overlap on O2 and the Cu1–O2–Cu2 angle is obtuse enough (115°).[19,20] In fact, there is no coupling as evidenced by the value of the Weiss constant ($|\Theta| < 1$ cm^{-1}). We think that the reason for this is probably to be found in the nonplanarity of the system. Actually, the N2–Cu2–O2 axis makes an angle of 129° with the Cu2 basal plane (O1, O1′, O4, O2). This situation is analogous to the folding of dihydroxy-bridged dicopper complexes, which is known to lead to smaller singlet–triplet gaps as a result of a decrease in both the ferromagnetic and the antiferromagnetic contributions to the exchange integral.[21]

In summary, this note reports the synthesis and the magnetic properties of new copper catecholates and describes the X-ray structural characterization of a novel mode of coordination of these ligands. Further work is currently in progress to fully characterize the redox properties of these compounds and study their reactivity.

Supplementary Material Available: Listings of anisotropic thermal parameters, interatomic distances and angles, and hydrogen atom coordinates (5 pages); a listing of observed and calculated structure factors (12 pages). Ordering information is given on any current masthead page.

---

(18) Nakamoto, K. *Infrared and Raman Spectra of Inorganic and Coordination Compounds*; Wiley: New York, 1978; pp 232, 246.
(19) Crawford, V. H.; Richardson, H. W.; Wasson, J. R.; Hodgson, D. J.; Hatfield, W. E. *Inorg. Chem.* **1976**, *15*, 2107–2110.
(20) Mikuriya, M.; Okawa, H.; Kida, S. *Bull. Chem. Soc. Jpn.* **1982**, *55*, 1086–1091.
(21) Kahn, O.; Charlot, M. F. *Nouv. J. Chim.* **1980**, *4*, 567–576.

Contribution from the Chemistry Division,
Oak Ridge National Laboratory, Oak Ridge, Tennessee 37831

Ammonolysis of Niobium(V) Bromide

L. Maya

Received October 2, 1986

The chemistry of transition-metal compounds in liquid ammonia is of interest because it provides an added perspective to the more extensively studied behavior of these compounds in aqueous systems. Ammonolytic reactions are more sensitive than the parallel hydrolytic processes to the polarizing power of the central atom and lead to a variety of products in which only a portion of the original ligands are displaced by amide. Hydrolysis, on the other hand, leads in general to fully hydroxo-substituted derivatives. However, in both cases, the products are susceptible to undergoing additional condensation through the formation of amido, imido, hydroxo, or oxo bridges.

The ammonolytic reactions can also be utilized as synthetic tools in providing oxygen-free derivatives containing strong metal–nitrogen bonds. It is in this area that our interest is focused since the derivatives can be used as intermediates to prepare precursors that can be thermally converted into advanced ceramic materials such as nitrides or carbonitrides.

Niobium nitrides and carbonitrides are materials with desirable properties such as hardness, thermal stability, and particularly, in the case of cubic forms, superconductivity.[1] The ammonolysis of niobium halides provides a synthetic route to the nitride. This has been previously examined by Fowles and Pollard,[2] who found, through tensimetric determinations, that the initial ammonolytic reaction leads to the ammonia-soluble derivative $NbCl_3(NH_2)_2$. Evaporation of the ammonia left a solid residue that, upon thermal treatment, produced NbN. Additional work by Allbutt and Fowles[3] showed that long-term ammonolysis leads to an insoluble residue having a formula corresponding to $NbBr(NH_2)_2NH$. (The structure of a similar tantalum analogue has been recently established.[4]) More recent developments in this area include the work of Sinitsyna,[5] who performed dry ammonolysis reactions between the niobium halides and an excess of the corresponding ammonium halide to produce niobium halide nitrides, $NbNX_2$. Finally, Grebtsova et al.[6] studied the thermal conversion of the ammonolysis residue of $NbCl_5$ into NbN by a variety of techniques.

The present work was undertaken to better characterize the ammonolytic intermediates as well as the thermal decomposition products and also to explore the use of these intermediates in the preparation of derivatives that could be converted into carbonitrides similar to previous work in the titanium system.[7]

---

(1) Toth, L. E. *Transition Metal Carbides and Nitrides*; Academic: New York, 1971.
(2) Fowles, G. W. A.; Pollard, F. H. *J. Chem. Soc.* **1952**, 4938.
(3) Allbutt, M.; Fowles, G. W. A. In *Developments in Inorganic Nitrogen Chemistry*; Colburn, C. B., Ed.; Elsevier: Amsterdam, 1966; Vol. 1.
(4) Bradley, D. C.; Hursthouse, M. B.; Abdul Malik, K. M.; Nielson, A. J.; ChotaVuru, G. B. *J. Chem. Soc., Dalton Trans.* **1984**, 1069.
(5) Sinitsyna, S. M. *Russ. J. Inorg. Chem.* (*Engl. Transl.*) **1977**, *22*, 402.
(6) Grebtsova, O. M.; Troitskii, V. N.; Shulga, Yu M. *J. appl. Chem. USSR* (*Engl. Transl.*) **1985**, *58*, 2011.
(7) Maya, L. *Inorg. Chem.* **1986**, *25*, 4213.

0020-1669/87/1326-1459$01.50/0